M 2 @C 79 N (M = Y, Tb): Isolation and Characterization of Stable Endohedral Metallofullerenes Exhibiting M−M Bonding Interactions inside Aza[80]fullerene Cages

ARTICLE *in* JOURNAL OF THE AMERICAN CHEMICAL SOCIETY · OCTOBER 2008

Impact Factor: 12.11 · DOI: 10.1021/ja802417d · Source: PubMed

8 AUTHORS, INCLUDING:

Liaosa Xu
Virginia Polytechnic Institute and State Univ…
19 PUBLICATIONS **755** CITATIONS
SEE PROFILE

Christine M Beavers
Lawrence Berkeley National Laboratory
96 PUBLICATIONS **1,854** CITATIONS
SEE PROFILE

Marilyn M. Olmstead
University of California, Davis
953 PUBLICATIONS **26,332** CITATIONS
SEE PROFILE

Alan Balch
University of California, Davis
597 PUBLICATIONS **19,169** CITATIONS
SEE PROFILE

Published in final edited form as:
J Am Chem Soc. 2008 October 1; 130(39): 12992–12997. doi:10.1021/ja802417d.

$M_2@C_{79}N$ (M = Y, Tb): Isolation and Characterization of Stable Endohedral Metallofullerenes Exhibiting M-M Bonding Interactions Inside Aza[80]Fullerene Cages

Tianming Zuo[++], **Liaosa Xu**[++], **Christine M. Beavers**[+], **Marilyn M. Olmstead**[+], **Wujun Fu**[++], **T. Daniel Crawford**[++], **Alan L. Balch**[+], and **Harry C. Dorn**[++]

+ *Department of Chemistry, University of California, Davis, One Shields Avenue, Davis, California 95616*

++ *Department of Chemistry, Virginia Polytechnic Institute and State University, Blacksburg, VA, 24061*

Abstract

$Y_2@C_{79}N$ and $Tb_2@C_{79}N$ have been prepared by conducting the Krätschmer-Huffman electric arc-process under 20 torr of N_2 and 280 torr of He with metal oxide doped graphite rods. These new heterofullerenes were separated from the resulting mixture of empty cage fullerenes and endohedral fullerenes by chemical separation and a two stage chromatographic process. Crystallographic data for $Tb_2@C_{79}N \cdot Ni(OEP) \cdot 2C_6H_6$ demonstrate the presence of an 80-atom cage with idealized I_h symmetry and two, widely separated Tb atoms inside with a Tb---Tb separation of 3.9020(10) Å for the major terbium sites. The EPR spectrum of the odd-electron $Y_2@C_{79}N$ indicates that the spin density largely resides on the two, equivalent yttrium ions. Computational studies on $Y_2@C_{79}N$ suggest that the nitrogen atom resides at a 665 ring junction in the equator on the fullerene cage and that the unpaired electron is localized in a bonding orbital between the two yttrium ions of this stable radical. Thus, the Tb-Tb bond length of the single-electron bond is the longest metal-metal bond reported so far.

Introduction

A number of reports of the detection and isolation of heterofullerenes, closed cages comprised of carbon atoms along with one or more non-carbon atoms arranged into five- and six-membered rings, have appeared.[1–3] Of these heterofullerenes, the mono-azafullerene derived from C_{60} by substituting a nitrogen atom for one of the carbon atoms, is the most thoroughly characterized.[4] Since the hypothetical $C_{59}N$ is an odd electron species, the neutral form of this mono-azofullerene is a dimer $\{C_{59}N\}_2$ with a single C-C bond connecting the two cages as seen in Scheme 1.[5] The corresponding monomeric cation, $[C_{59}N]^+$, is isoelectronic with C_{60} and is a stable species that has been isolated in crystalline form as salts with various counter anions.[6]

Fullerenes themselves can act as hosts that encapsulate other atoms, molecules or atomic clusters. The resulting endohedral fullerenes have attracted considerable attention because the entrapped atoms bring with them an array of useful physical properties. For example, endohedral fullerenes with paramagnetic metal ions firmly trapped inside have been considered promising candidates for the next generation of contrast agents for magnetic resonance imaging (MRI).[7–10] Similarly, endohedrals may be used to deliver radioactive atoms for applications in nuclear medicine.[11,12]

Correspondence to: Alan L. Balch.

There has been only a limited amount of consideration given to the possibility that heterofullerenes could encapsulate other atoms or molecules. Theoretical work has considered the electronic structural properties that would result from substitution of carbon atoms in known endohedrals by heteroatoms like nitrogen or boron.[13,14] Experimental observations on such heterofullerene endohedrals appears to be limited to a single report that describes the formation of species purported to be $[La@C_{81}N]^+$ and $[La_2@C_{79}N]^+$, that were formed by fast atom bombardment mass fragmentation of the adducts, $La@C_{82}NCH_2Ph$ and $La_2@C_{80}NCH_2Ph$.[15] This report also contained the results of electronic structure calculations on the corresponding neutral molecules that supported the formulation of these heteroendohedrals. In particular these computations suggested that the neutral molecules, $La@C_{81}N$ and $La_2@C_{79}N$, would exist as monomers and that the added electron that results from the nitrogen substitution would be transferred to the metal centers within the cage.

Subsequent to the report describing $[La@C_{81}N]^+$ and $[La_2@C_{79}N]^+$, it has become clear that a number of different types of clusters of atoms can be found inside fullerene cages. Thus, there are large families of endohedrals built about generally planar M_3N units,[16–18] of which the prototype is $Sc_3N@I_h$-C_{80}.[19] Additionally there is a class of endohedrals that involves an M_xC_2(x = 2 ~ 3) unit encased in a fullerene cage. Examples of these carbide containing endohedrals include $Sc_2C_2@C_{84}$[20] and $Sc_3C_2@I_h$-C_{80}.[21] As a result, it is possible that a molecule having the composition $La_2C_{79}N$ could have any of the following structures: $La_2NC@C_{78}$, $La_2C_2@C_{77}N$, or $La_2@C_{79}N$.

Here we report the preparation and isolation of sufficient quantities of $M_2@C_{79}N$ (M = Y, Tb) to allow structural characterization.

Results

Preparation and Isolation

Samples of the dimetallic aza[80]fullerenes, $M_2@C_{79}N$ (M = Tb or Y) were prepared utilizing the well established Krätschmer-Huffman (K-H) electric arc-process under 20 torr of N_2 and 280 torr of He to vaporize cored graphite rods that were packed with Y_2O_3 or Tb_4O_7.[16] The toluene-soluble extract from the electric-arc generator was separated first based on chemical reactivity differences using a cyclopentadiene-functionalized Merrifield peptide resin (CPDE-MPR) column and then further purified by two-stage HPLC chromatography as previously described.[16,22,23] There were seven fractions from the 5PBB column at the first-stage of HPLC. The initially eluting fraction contained $M_2@C_{79}N$ and C_{84}. $M_2@C_{79}N$ was further separated from C_{84} on a 5PYE column in the second-stage of HPLC. The HPLC chromatograms and mass spectra establish the identity of the purified samples of $Y_2@C_{79}N$ and $Tb_2@C_{79}N$ and the presence of a nitrogen atom in $Tb_2@C_{79}N$ was confirmed by the MS spectrum of ^{15}N-labeled sample (see supporting information).

The close correspondence between the UV/vis spectra of $Y_2@C_{79}N$ and $Tb_2@C_{79}N$ and the similar chromatographic retention behavior of $Y_2@C_{79}N$ and $Tb_2@C_{79}N$ suggests close correspondence of the cage electronic polarizabilities that are not significantly influenced by the nature of the internal M_2 cluster. It is also well recognized that the chromatographic capacity factor is proportional to the fullerene cage polarizability and that it has a simple linear relationship with the fullerene cage size or carbon number. The retention mechanism is generally proportional to the fullerene cage polarizability and is dominated by π-π interactions with the stationary phase.[24–26] Thus, the elution profile (co-elution with empty cage C_{84}, see SI) of $M_2@C_{79}N$ suggests charge transfer to the cage surface representing to a first approximation 84–85 π-electrons. This surface charge is consistent with the computational model of $[M_2]^{5+}@[C_{79}N]^{5-}$ (M = Y or Tb) (*vide infra*).

Crystallographic Studies

Black prisms of $Tb_2@C_{79}N \cdot Ni(OEP) \cdot 2C_6H_6$ were obtained by cocrystallization of $Tb_2@C_{79}N$ and Ni(OEP) (OEP is the dianion of octaethylporphyrin) from a benzene solution of the components. Data were collected at a synchrotron source and refined by standard procedures. A drawing of the molecule obtained from the crystallographic data is shown in Figure 4. The crystallographic data are completely consistent with the $Tb_2@C_{79}N$ formulation for the molecule and definitively rule out the alternative possibilities that the molecule could be $Tb_2CN@C_{78}$ or $Tb_2C_2@C_{77}N$. The results demonstrate the presence of an 80-atom cage with idealized I_h symmetry and two, widely separated Tb atoms inside with a Tb-Tb separation of 3.9020(10) Å for the major terbium sites. Each Tb atom coordinates with an adjacent hexagon of the cage in η^6-fashion. The Tb-C distances range from 2.366(10) to 2.523(11) Å with the Tb to ring centroid distance of 1.969(10) Å. The placement of the Tb atoms above the hexagons is remarkably similar to the location of the three Tb atoms in $Tb_3N@C_{80}$-I_h, where the Tb-C distances range from 2.404(3) to 2.518(3) Å and the Tb to ring centroid distance is 1.975(3) Å.[16]

As is typical with structures of this sort,[16,19,23] there is disorder in the cage orientation and the locations of the Tb atoms inside. Only the major orientation is shown in Figure 1, but there are two orientations of the cage and ten other partially occupied sites for the terbium atoms. Another cage orientation and the locations of all terbium sites are shown in Figure 2. The multiplicity of terbium sites within the cage suggest that there is a low barrier to re-orientation of the Tb_2 unit with regard to the cage itself. Similarly the Sc_3N unit within $Sc_3N@C_{80}$ was found to possess a low barrier for re-orientation.[27] As a result of the disorder, the crystallographic data do not identify specifically the site of the nitrogen atom in the cage. Because of the similar sizes and scattering power of carbon and nitrogen, differentiation between these two atoms is challenging in such a high symmetry environment. The X-ray crystal structure of the carbocation, $(C59N)^+$, also displays disorder in the position of the nitrogen atom.[6]

The possibility that there is a specific interaction between the nitrogen atom of the cage and the Ni(OEP) molecule has also been examined and excluded. The closest contacts of atoms of the cage with the nickel atom are 3.044(8) and 2.805(3) Å for the two cage orientations. These distances are within the range found for numerous analogous structures with all-carbon cages.[2]

Electron Paramagnetic Resonance Studies

$Y_2@C_{79}N$ contains an odd number of electrons and the paramagnetic character of $Y_2@C_{79}N$ was confirmed by X-band EPR solution measurements at 298 K as illustrated in Figure 3. For a dilute sample in toluene solution three symmetric lines with a 1:2:1 intensity ratio were observed. This pattern is consistent with hyperfine splitting due to two equivalent ^{89}Y nuclides (100 % natural abundance, nuclear spin of ½). The observed g factor, $g = 1.9740$ and large observed yttrium coupling of |81.23| G indicates that there is significant unpaired spin density localized on the yttrium centers. No hyperfine coupling was observed due to the nitrogen atom. The isotropic yttrium coupling of |81.23| G for $Y_2@C_{79}N$ is larger than the anisotropic coupling constants obtained for Y_3 clusters in frozen argon matrices by Knight and coworkers.[28] The spectra of the Y_3 cluster revealed two equivalent yttrium centers with $a_{||} = 27.7$ G and $a\perp = 14.5$ G and a second yttrium center with $a_{||} = 27.7$ G and $a_{||} = 19.7$ G. The yttrium coupling for $Y_2@C_{79}N$ has a greater magnitude than those observed for $[Y_3N@I_h\text{-}C_{80}C_4H_9N]^-$, which had an isotropic hyperfine splitting of |6.26| G for two equivalent yttrium centers and an isotropic hyperfine splitting of |1.35| G for a third inequivalent yttrium center.[29] The isotropic g factors for $Y_2@C_{79}N$ (1.9740) and $[Y_3N@I_h\text{-}C_{80}C_4H_9N]^-$(1.998915) and the anisotropic g factors for the Y_3 cluster ($g_{||} = 1.9603$ and $g\perp = 1.9578$) are all below 2 and are indicative of significant

spin density on the yttrium centers in each of these clusters. These results are in sharp contrast to the isotropic g factor and hyperfine coupling reported for the metallofullerene $Y@C_{82}$ (a = 0.49 G, g = 2.0006) where the unpaired electron spin density is mainly delocalized on the carbon cage.[30]

A solid sample of $Y_2@C_{79}N$ exhibits an EPR spectrum consisting of a single line, which is broadened due to Heisenberg exchange. The effect of Heisenberg exchange was confirmed by a solid-state dilution experiment where the $Y_2@C_{79}N$ sample was mixed with an empty cage fullerene, C_{84}, of similar size. In this experiment, a set of three symmetric resonances in a 1:2:1 intensity ratio was observed as illustrated in Figure 3. The hyperfine coupling and g factor were similar to the data obtained from a toluene solution. The appearance of the EPR spectrum of the mixed solid solution suggests nearly isotropic motion of the $Y_2@C_{79}N$ molecule and/or Y-Y cluster motional averaging in the C_{84} solid matrix. It is also important to note that the EPR spectrum for the $Y_2@C_{79}N$ sample was unchanged after 6 months (even when exposed to O_2). Thus, this paramagnetic molecule possesses considerable chemical stability.

An EPR spectrum for the $Tb_2@C_{79}N$ sample was not observed. The lack of a readily detected EPR spectrum is consistent with the well-recognized, short electron relaxation time for the Tb^{+3} ion.[31,32]

Computational Studies

In order to augment the experimental observations and assist in explaining some of the physical properties of these new azafullerene endohedrals, density functional theory (DFT) computations using the spin-unrestricted B3LYP functional as defined in the Gaussian 03[33] program package[34–36] were performed for $Y_2@C_{79}N$ as a suitable prototype. In the I_h-C_{80} cage there are two types of carbon atoms: 60 carbon atoms reside in pentagons at a 665 junction, while the remaining 20 are not part of pentagons but reside at the junctions of three hexagons (a 666 junction) as can be seen in Figure 4. In order to define further the location of the nitrogen atom in the $C_{79}N$ cage, UB3LYP geometry optimizations using the DZVP basis set for Y[37] and the 6-31G* basis set for C and N[38] were carried out with the nitrogen atom located at the two possible sites on the cage surface that are shown in Figure 4. Each isomer was demonstrated to be a minimum on the potential energy hypersurface via analytic second derivative (harmonic vibrational frequency) calculations. Our computational results for $Y_2@C_{79}N$ predict that the 665 isomer shown in Part A of Figure 4 is 13.3 kcal/mol more stable than the 666 isomer. The HOMO-LUMO gaps are relatively large for both isomers at ca. 2.4 eV. 39-42These values are similar to the HOMO-LUMO gaps for the well known $M_3N@I_h$-C_{80} class.[39–42] similar computational approach for the empty $[C_{79}N]^{5-}$ cage also predicts significantly higher thermodynamic and kinetic stability for the (665) isomer in comparison with the (666) isomer.

Figure 5 shows the UB3LYP molecular orbital energies for the orbitals near the HOMO-LUMO gap for three related species: even-electron $Y_2@I_h$-C_{80}, and odd-electron $[Y_2@I_h$-$C_{80}]^-$ obtained by one-electron reduction of $Y_2@I_h$-C_{80}, and $Y_2@C_{79}N$. The latter two are isoelectronic. The computational results for $Y_2@I_h$-C_{80} indicate that it is a small band-gap material with a HOMO-LUMO gap of 0.82 eV. This small gap suggests this endohedral will have low stability, a result that is consistent with the paucity of observed experimental quantities of the $Y_2@I_h$-C_{80}.

In contrast, iso-electronic $[Y_2@I_h$-$C_{80}]^-$ and $Y_2@C_{79}$Nare predicted by the spin-unrestricted B3LYP approach to be large band-gap materials with the electron spins residing in orbitals that are localized between the yttrium ions. By comparing the shapes of the UB3LYP molecular orbitals, it is recognized that the low-lying HOMO-4 orbital of $[Y_2@I_h$-$C_{80}]^-$ originates from the LUMO of $Y_2@I_h$-C_{80}. Upon accepting one electron, the LUMO in Y2@I_h-C80 becomes the HOMO-4 orbital of $[Y_2@I_h$-$C_{80}]^-$. The small HOMO-LUMO gap (0.82 eV) of $Y_2@I_h$-

C_{80}evolves as the large HOMO-LUMO gap (2.53 eV) of $[Y_2@I_h\text{-}C_{80}]^-$ as shown in Figure 5. As such, this system violates the Aufbau principle. However, there are precedents in spin-unrestricted calculations where spin-polarized orbitals reside at lower energy than the HOMO.[43,44] Additionally, photoelectron spectroscopy has provided experimental evidence for the occurrence of a spin-containing orbital that resides at lower energy than the HOMO.[45] (We note that, in contrast to the above, spin-restricted B3LYP calculations place the singly occupied orbital higher in energy than all other occupied orbitals. However, both the RB3LYP and UB3LYP models agree as to the size of the HOMO-LUMO gap and the shapes of the relevant valence MOs.)

The B3LYP/DZVP(Y)+6-31G*(C,N) model produces a calculated yttrium hyperfine coupling of −62.4 G for the 665 isomer (−61.2 G for the 666 isomer), which is consistent with the large α spin density observed between the two yttrium atoms in the cluster and compares well with the observed yttrium coupling constant of |81.23| G. The lack of an observed ^{14}N hyperfine coupling for the cage nitrogen atom in the observed EPR spectrum is consistent with the small calculated value for the nitrogen hyperfine coupling of 0.01 G.

The computed Y-Y separation for $Y_2@C_{79}N$ is 3.994 Å. This is unusually long for a molecule in which computations suggest that a one-electron bond connects the two yttrium ions. However, this distance is rather similar to the Tb-Tb distance of 3.9020(10) Å for the major terbium site in $Tb_2@C_{79}N$. Electrostatic repulsion within these M_2^{5+} units is likely to play a major role in determining the M-M separations.

In order to ensure that the DZVP basis set for Y used in the above calculations is sufficiently complete to provide a realistic description of the fullerene, we carried out a re-contraction of the correlation-consistent triple-zeta (cc-pVTZ) basis set using the exponents developed by Peterson and co-workers for Douglas-Kroll relativistic calculations.[46] Using diffuse functions taken from the aug-cc-pVTZ-DK published by Peterson *et al.* to define an aug-cc-pVTZ basis for Y, we have carried out single-point calculations at the B3LYP/aug-cc-pVTZ(Y)+6-31G*(C,N) level of theory. We find that the results are essentially identical to those reported above using the DZVP basis set for Y, including the energy difference between the 665 and 666 isomers of $Y_2@C_{79}N$ (13.2 kcal/mol), the HOMO-LUMO gap, and the yttrium hyperfine coupling (−59.7 G).

Discussion and Conclusions

The results presented here demonstrate that significant quantities of $Y_2@C_{79}N$ and $Tb_2@C_{79}N$ were formed along with a range of endohedrals of the $M_3N@C_{2n}$ class and empty cage fullerenes when the Krätschmer-Huffman electric arc-process was conducted under 20 torr of N2 and 280 torr of He. Y2@C79N and Tb2@C79N are soluble species that can be separated from other fullerene and endohedral fullerene molecules by chromatographic means. The crystallographic data for Tb2@C79N clearly reveal the presence of a monomeric endohedral. Tb2@C79N consists of a cage of 80 atoms built with an atomic arrangement similar to that of $I_h\text{-}C_{80}$ with two widely separated (3.9020(10) Å) terbium ions inside. While the crystallographic data do not locate the specific position of the nitrogen atom on the cage, our computational studies indicate that the nitrogen atom is probably located within a pentagon at a 665 site in the equatorial mirror plane that is orthogonal to the line between the two terbium ions as seen in Figure 4. Similarly, computational studies on $La_2@C_{79}N$ also came to the conclusion that the nitrogen atom would reside at a 665 site symmetrically displaced between the two metal ions.[15] Although we did not isolate the significant amount of pure $La_2@C_{79}N$ for characterization, our high resolution LD-TOF mass spectrum clearly shows the existence of $La_2@C_{79}N$, along with $La@C_{81}N$ (see supporting information).

The EPR spectrum of $Y_2@C_{79}N$ are consistent with a stable heterofullerene radical with a *g*-factor and yttrium hyperfine coupling that indicate that there is a significant amount of spin density localized on the two equivalent yttrium ions. The computational studies are consistent with these observations and indicate that the odd electron resides in an unusual bonding orbital that is localized between the two yttrium ions. The combination of our crystallographic and EPR data as well as theoretical calculation results demonstrates that the single-electron bond between two metal ions inside the $[C_{79}N]^{5-}$ heterofullerene cage is the longest metal-metal bond reported so far.[47–49]

Experimental

Synthesis of $Y_2@C_{79}N$ and $Tb_2@C_{79}N$

Core-drilled graphite rods (6.4 mm in diameter by152 mm in length) were packed with a mixture of Y_2O_3 or Tb_4O_7, graphite powder and iron nitride (FexN, x = 2 ~ 4). The total M:C molar ratios were about 3:100. The packed rods were pre-heated to about 1000°C under a flow of dinitrogen for about 10 hours to remove air and moisture. The rods were then vaporized in a Krätschmer -Huffman arc-discharge fullerene generator filled with a mixture of 20 Torr dinitrogen and 280 Torr helium gases. For ^{15}N-labelled sample, $^{15}N_2$ was used instead of natural dinitrogen gas.The raw soot produced in the reactor was extracted in a Soxhlet extractor using toluene as solvent for approximately 20 hours. The resulting extract was initially separated utilizing a CPDE-MPR column as previously described.[16] With chemical separation, most of the empty cages and reactive classical endofullerenes are retained on the CPDE-MPR column and thus cannot be eluted. The HPLC chromatograms of the yttrium and terbium samples before and after chemical separation are shown in the supporting information.

In the case of yttrium, seven fractions were separated. The initially eluting fraction, Y1, contained $Y_2@C_{79}N$ and C_{84}. After chemical separation, the terbium-based sample had a similar HPLC trace, and also was separated into seven fractions. The first fraction, Tb1, contained $Tb_2@C_{79}N$ and C_{84}. Fractions Y1 and Tb1 were collected and were further separated using a 5PYE column. C_{84} was easily separated from $Y_2@C_{79}N$ (or $Tb_2@C_{79}N$) since their retention times on a 5PYE column were very different. The HPLC chromatograms of the pure $Y_2@C_{79}N$ and $Tb_2@C_{79}N$ samples are shown in Figure 1.

X-ray Crystallography and Data Collection

The crystals were removed from the glass tubes in which they were grown together with a small amount of mother liquor, placed on a microscope slide together with a small amount of mother liquor, and immediately coated with a hydrocarbon oil. Suitable crystals were mounted on glass fibers with silicone grease. Data were collected at beamline 11.3.1 at the Advanced Light Source with the use of 0.7749 Å synchrotron radiation and a Bruker Platinum 200 goniometer. All data sets were integrated with the Bruker SAINT (v.7.16) program. Crystal data are reported below. A semi-empirical absorption correction utilizing equivalents was employed.[50] The structure was solved by direct methods and refined using all data (based on F^2) using the software of SHELXTL 5.1. Hydrogen atoms were located in a difference map, added geometrically, and refined with a riding model.

Crystal data—$Tb_2@C_{80}N{\cdot}Ni(OEP)\cdot 2$benzene, black prism (0.07 × 0.12 × 0.15 mm) of $C_{128}H_{56}N_4NiTb2$, Mw = 2026.32, monoclinic, space group C2/m, a = 25.1848(7) Å, b = 15.1160(5) Å, c = 19.7406(7) Å, β = 95.063(1)°, V = 7485.8(4) Å^3 at 90(2) K, γ = 0.77490 Å, ∝= 2.727 mm^{-1}, Z = 4. Refinement of 10012 reflections, 568 parameters and 1 restraint yielded wR2 = 0.243 for all data and a conventional R_1 of 0.0844 based on 8915 reflections with I > 2σ(I).

Supplementary Material

Refer to Web version on PubMed Central for supplementary material.

Acknowledgments

We thank the National Science Foundation [CHE-0413857 (A.L.B.), CHE-0443850 (H.C.D.), DMR-0507083 (H.C.D.), CHE-0715185 (T.D.C)] and the National Institute of Health [1R01-CA119371-01 (H.C.D.)] for support. The authors gratefully acknowledge the Advanced Light Source, Beamline 11.3.1, operated under the auspices of the Director, Office of Science, Office of Basic Energy Sciences of the U.S. Department of Energy under Contract No. DE-AC02-05CH11231. We thank Mr. Kim Harich, Ms Anne Campbell, and Dr. Keith Ray for the mass spectra. We are also grateful to Prof. Kirk Peterson of Washington State University for providing the re-contracted cc-pVTZ basis set for yttrium used in the computational studies.

References

1. Vostrowsky O, Hirsch A. Chem Rev 2006;106:5191–5207. [PubMed: 17165685]
2. Branz W, Billas IML, Malinowski N, Tast F, Heinebrodt M, Martin TP. J Chem Phys 1998;109:3425.
3. Poblet JM, Winkler K, Cancilla M, Hayashi A, Lebrilla CB, Balch AL. Chem Comm 1999:493.
4. Hirsch A, Nuber B. Accounts Chem Res 1999;32:795.
5. Hummelen JC, Knight B, Pavlovich J, Gonzalez R, Wudl F. Science 1995;269:1554–6. [PubMed: 17789446]
6. Kim KC, Hauke F, Hirsch A, Boyd PDW, Carter E, Armstrong RS, Lay PA, Reed CA. J Am Chem Soc 2003;125:4024. [PubMed: 12670204]
7. Mikawa M, Kato H, Okumura M, Narazaki M, Kanazawa Y, Miwa N, Shinohara H. Bioconjugate Chem 2001;12:510–514.
8. Bolskar RD, Benedetto AF, Husebo LO, Price RE, Jackson EF, Wallace S, Wilson LJ, Alford JM. J Am Chem Soc 2003;125:5471–5478. [PubMed: 12720461]
9. Tóth E, Bolskar RD, Borel A, González G, Helm LEMA, Sitharaman B, Wilson LJ. J Am Chem Soc 2005;127:799–805. [PubMed: 15643906]
10. Fatouros PP, Corwin FD, Chen ZJ, Broaddus WC, Tatum JL, Kettenmann B, Ge Z, Gibson HW, Russ JL, Leonard AP, Duchamp JC, Dorn HC. Radiology 2006;240:756. [PubMed: 16837672]
11. Wilson LJ, Cagle DW, Thrash TP, Kennel SJ, Mirzadeh S, Alford JM, Ehrhardt GJ. Coord Chem Rev 1999;192:199–207.
12. Li QN, Xiu Y, Zhang XD, Liu RL, Du QQ, Shun XG, Chen SL, Li WX. Nucl Med Biol 2002;29:707–710. [PubMed: 12234597]
13. Hou JQ, Kang HS. Chem Phys 2007;334:29.
14. Hou JQ, Kang HS. J Phys Chem A 2007;111:1111. [PubMed: 17253661]
15. Akasaka T, Okubo S, Wakahara T, Yamamoto K, Kobayashi K, Nagase S, Kato T, Kako M, Nakadaira Y, Kitayama Y, Matsuura K. Chem Lett 1999:945.
16. Zuo T, Beavers CM, Duchamp JC, Campbell A, Dorn HC, Olmstead MM, Balch AL. J Am Chem Soc 2007;129:2035–2043. [PubMed: 17256857]
17. Dunsch L, Yang S. Small 2007;3:1298. [PubMed: 17657757]
18. Melin F, Chaur MN, Engmann S, Elliott B, Kumbhar A, Athans AJ, Echegoyen L. Angew Chem Int Ed 2007;46:9032.
19. Stevenson S, Rice G, Glass T, Harlch K, Cromer F, Jordan MR, Craft J, Hadju E, Bible R, Olmstead MM, Maltra K, Fisher AJ, Balch AL, Dorn HC. Nature 1999;401:55–57.
20. Wang CR, Kai T, Tomiyama T, Yoshida T, Kobayashi Y, Nishibori E, Takata M, Sakata M, Shinohara H. Angew Chem Int Ed 2001;40:397.
21. Liduka Y, Wakahara T, Nakahodo T, Tsuchiya T, Sakuraba A, Maeda Y, Akasaka T, Yoza K, Horn E, Kato T, Liu MTH, Mizorogi N, Kobayashi K, Nagase S. J Am Chem Soc 2005;127:12500. [PubMed: 16144392]
22. Ge Z, Duchamp JC, Cai T, Gibson HW, Dorn HC. J Am Chem Soc 2005;127:16292. [PubMed: 16287323]

23. Beavers CM, Zuo T, Duchamp JC, Harich K, Dorn HC, Olmstead MM, Balch AL. J Am Chem Soc 2006;128:11352–11353. [PubMed: 16939248]
24. Zuo TM, Olmstead MM, Beavers CM, Balch AL, Wang GB, Yee GT, Shu CY, Xu LS, Elliott B, Echegoyen L, Duchamp JC, Dorn HC. Inorganic Chemistry 2008;47:5234–5244. [PubMed: 18447327]
25. Fuchs D, Rietschel H, Michel RH, Fischer A, Weis P, Kappes MM. Journal of Physical Chemistry 1996;100:725–729.
26. Stevenson S, Burbank P, Harich K, Sun Z, Dorn HC, van Loosdrecht PHM, deVries MS, Salem JR, Kiang CH, Johnson RD, Bethune DS. Journal of Physical Chemistry A 1998;102:2833–2837.
27. Campanera JM, Bo C, Olmstead MM, Balch AL, Poblet JM. J Phys Chem A 2002;106:12356–12364.
28. Knight LB Jr, Woodward RW, Van Zee RJ, Weltner W Jr. J Chem Phys 1983;79:5820–7.
29. Echegoyen L, Chancellor CJ, Cardona CM, Elliot B, Rivera J, Olmstead MM, Balch AL. Chem Commun 2006:2653.
30. Kikuchi K, Nakao Y, Suzuki S, Achiba Y, Suzuki T, Maruyama Y. J Am Chem Soc 1994;116:9367–8.
31. Wortman DE. Phys Rev 1968;175:488–98.
32. Gafurov MR, Ivanshin VA, Kurkin IN, Rodionova MP, Keller H, Gutmann M, Staub U. J Magn Reson 2003;161:210–4. [PubMed: 12713972]
33. Frisch, MJ., et al. Gaussian, Inc; Wallingford, CT: 2004.
34. Becke AD. J Chem Phys 1993;98:5648.
35. Lee C, Yang W, Parr RG. Phys Rev B 1988;37:785.
36. Stephens PJ, Devlin FJ, Chabalowski CF, Frisch MJ. J Phys Chem 1994;98:11623.
37. Godbout N, Salahub DR, Andzelm J, Wimmer E. Can J Chem 1992;70:560.
38. Hehre WJ, Ditchfield R, Pople JA. J Chem Phys 1972;56:2257.
39. Cai T, Xu L, Anderson MR, Ge Z, Zuo T, Wang X, Olmstead MM, Balch AL, Gibson HW, Dorn HC. J Am Chem Soc 2006;128:8581–8589. [PubMed: 16802825]
40. Iiduka Y, Ikenaga O, Sakuraba A, Wakahara T, Tsuchiya T, Maeda Y, Nakahodo T, Akasaka T, Kako M, Mizorogi N, Nagase S. J Am Chem Soc 2005;127:9956–9957. [PubMed: 16011332]
41. Dunsch L, Krause M. ChemPhysChem 2004;5:1445–1449. [PubMed: 15499866]
42. Elliott B, Yu L, Echegoyen L. J Am Chem Soc 2005;127:10885–10888. [PubMed: 16076194]
43. Wu X, Lu X. J Am Chem Soc 2007;129:2171–2177. [PubMed: 17256861]
44. Cloke FGN, Green JC, Kalysoyannis N. Organometallics 2004;23:832.
45. Westcott BL, Gruhn NE, Michelson LJ, Lichtenberger DL. J Am Chem Soc 2000;122:8083.
46. Peterson KA, Figgen D, Dolg M, Stoll H. J Chem Phys 2007;126:124101. [PubMed: 17411102]
47. Cotton FA, Koch SA, Millar M. Inorg Chem 1978;17:2084.
48. Kreisel KA, Yap GPA, Dmitrenko O, Landis CR, Theopold KH. J Am Chem Soc 2007;129:14162. [PubMed: 17967028]
49. Green SP, Jones C, Stasch A. Science 2007;318:1754–1757. [PubMed: 17991827]
50. Sheldrick GM. SADABS 2.10. Acta Crystallogr Sect A 1995;A51:33.

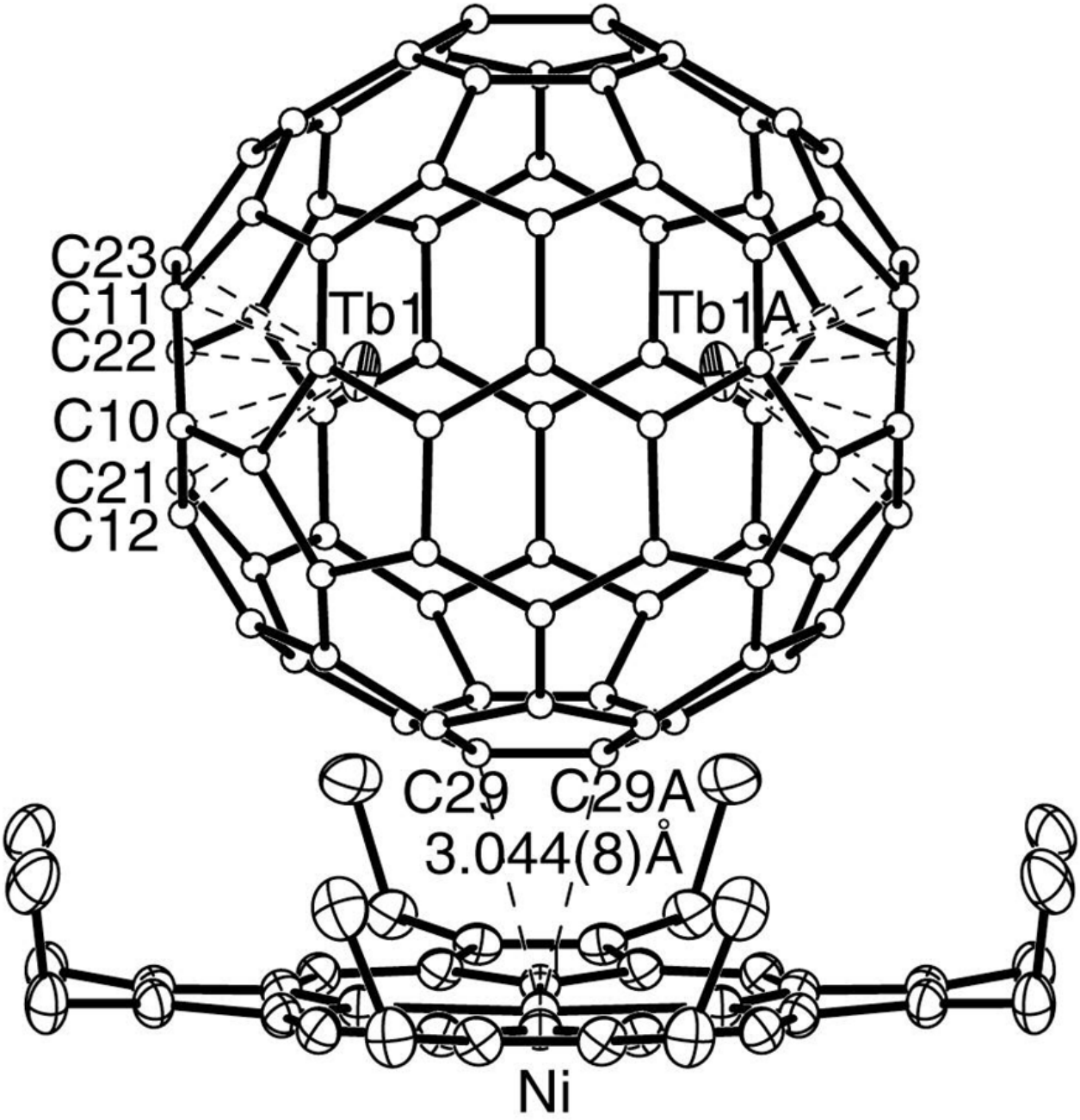

Figure 1.

A drawing of the crystallographically determined structure of $Tb_2@C_{79}N$, Only the symmetrical molecular site with 0.050 fractional occupancy is shown. At this site there is a crystallographic mirror plane which lies perpendicular to the plane of the paper and bisects the line between the two terbium atoms. The Tb1-Tb1A separation in 3.9020(10) and the occupancy of Tb1 corresponds to 0.43 of the total Tb content.

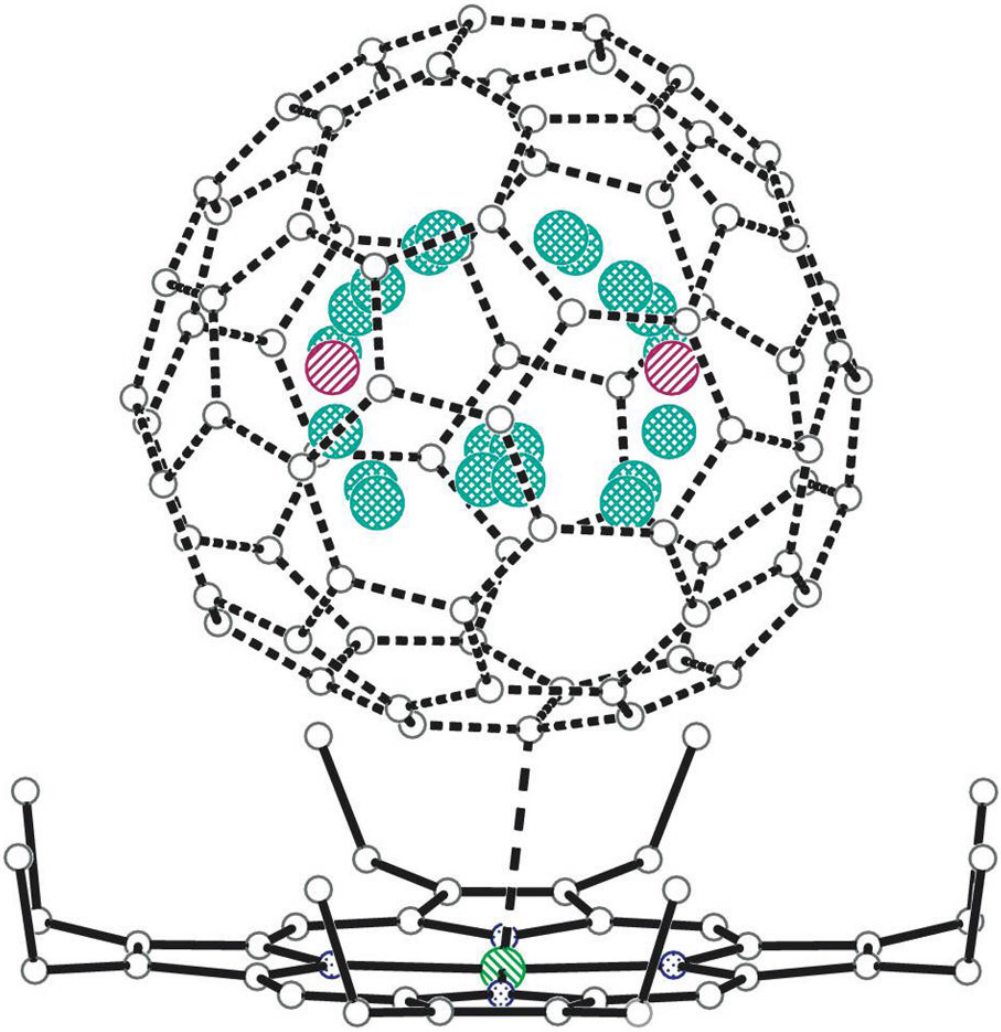

Figure 2.

A drawing of the crystallographically determined structure of $Tb_2@C_{79}N$ showing the unsymmetrical orientation of the heterofullerene cage. The orientation shown here has 0.25 fractional occupancy and a symmetry-related orientation generated by the crystallographic mirror plane has 0.25 occupancy. All of the terbium atom positions are shown along with those generated by the crystallographic mirror plane. The sites Tb2 through Tb11 have fractional occupancies that range from 0.102 to 0.026. When summed, these represent 0.57 of the total terbium content, while Tb1 (shown in red and hidden behind another terbium site) represents 0.43 of the terbium content in the asymmetric unit. The shortest contact (2.805(3) Å) between a cage atom and the nickel ion in the porphyrin is indicated by a dashed line.

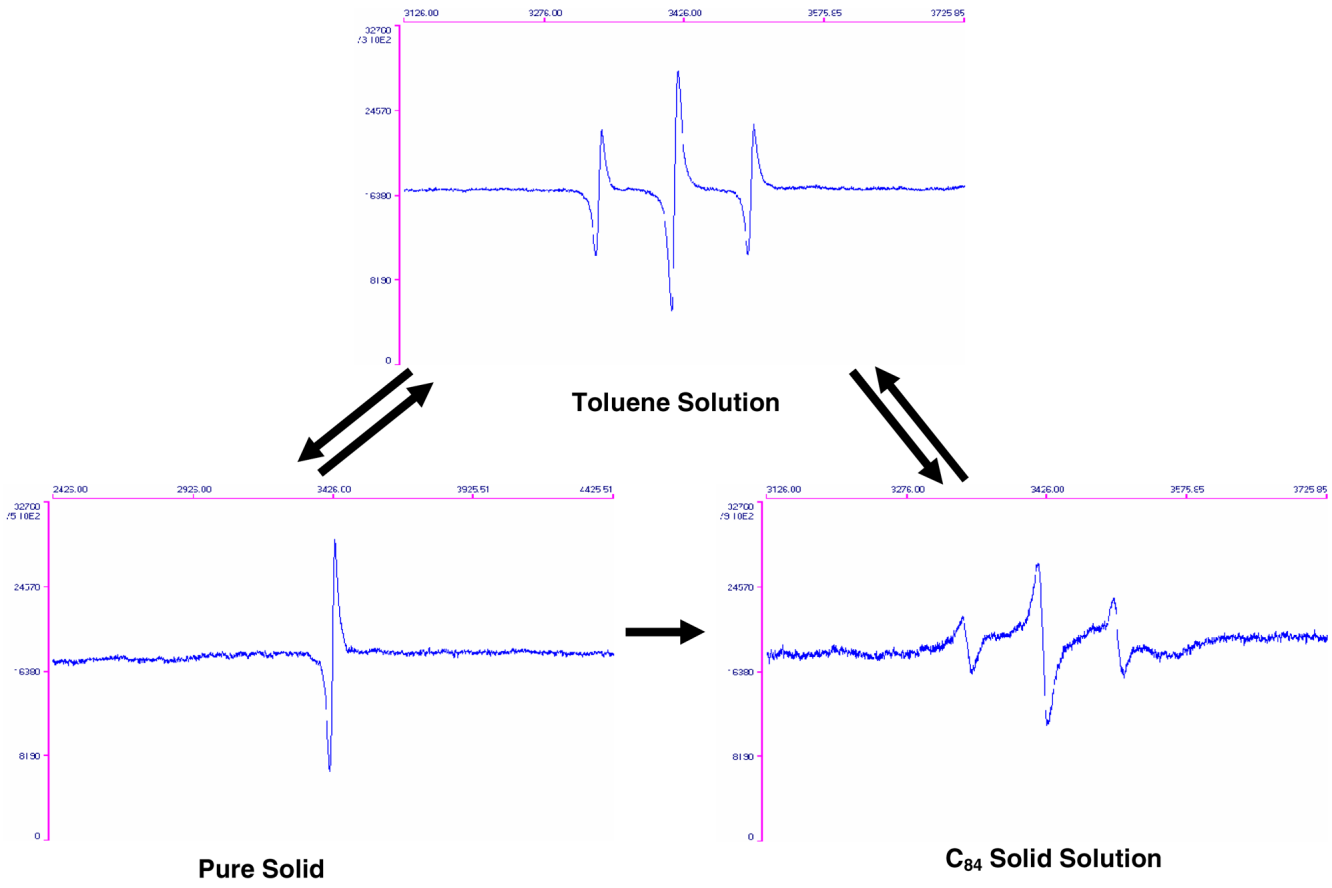

Figure 3.

ESR spectra of $Y_2@C_{79}N$ samples in toluene solution, as a solid, and as a solid solution with C_{84}.

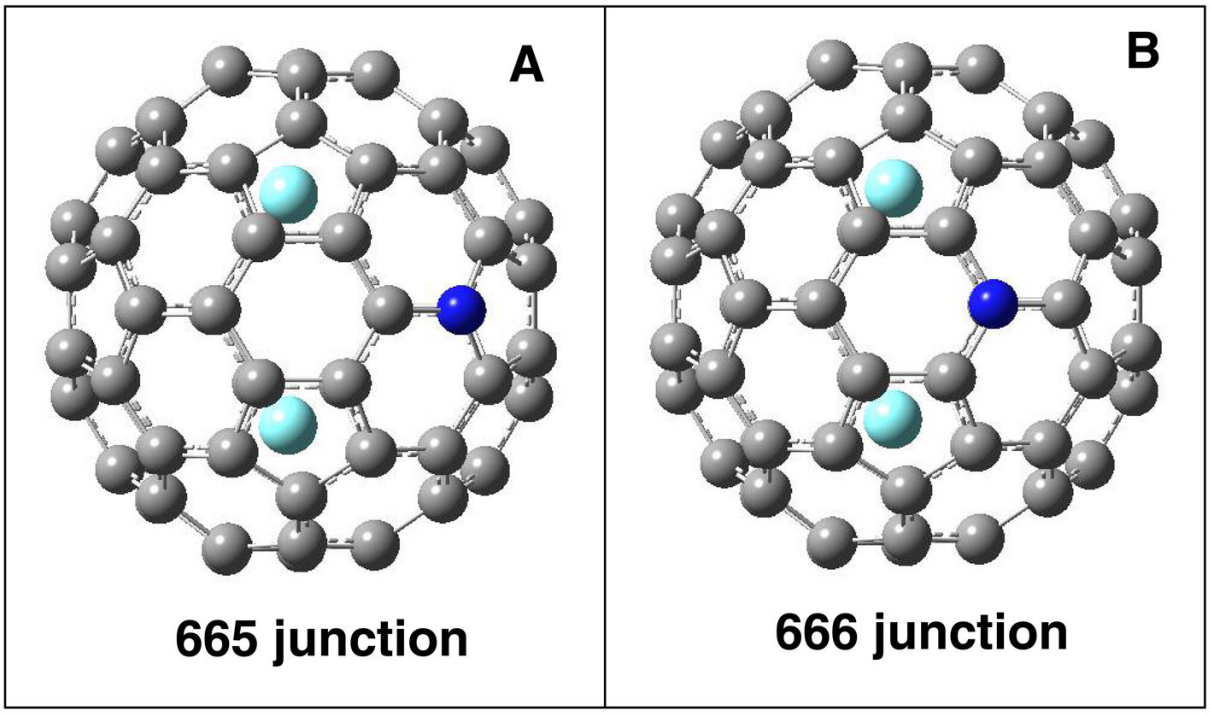

Figure 4.
Illustrations of the computed structures of $Y_2@C_{79}N$ with the nitrogen atom replacing: (A) a carbon atom in a pentagon (a 665 junction) and (B) a carbon atom that is not in a pentagon (a 666 junction).

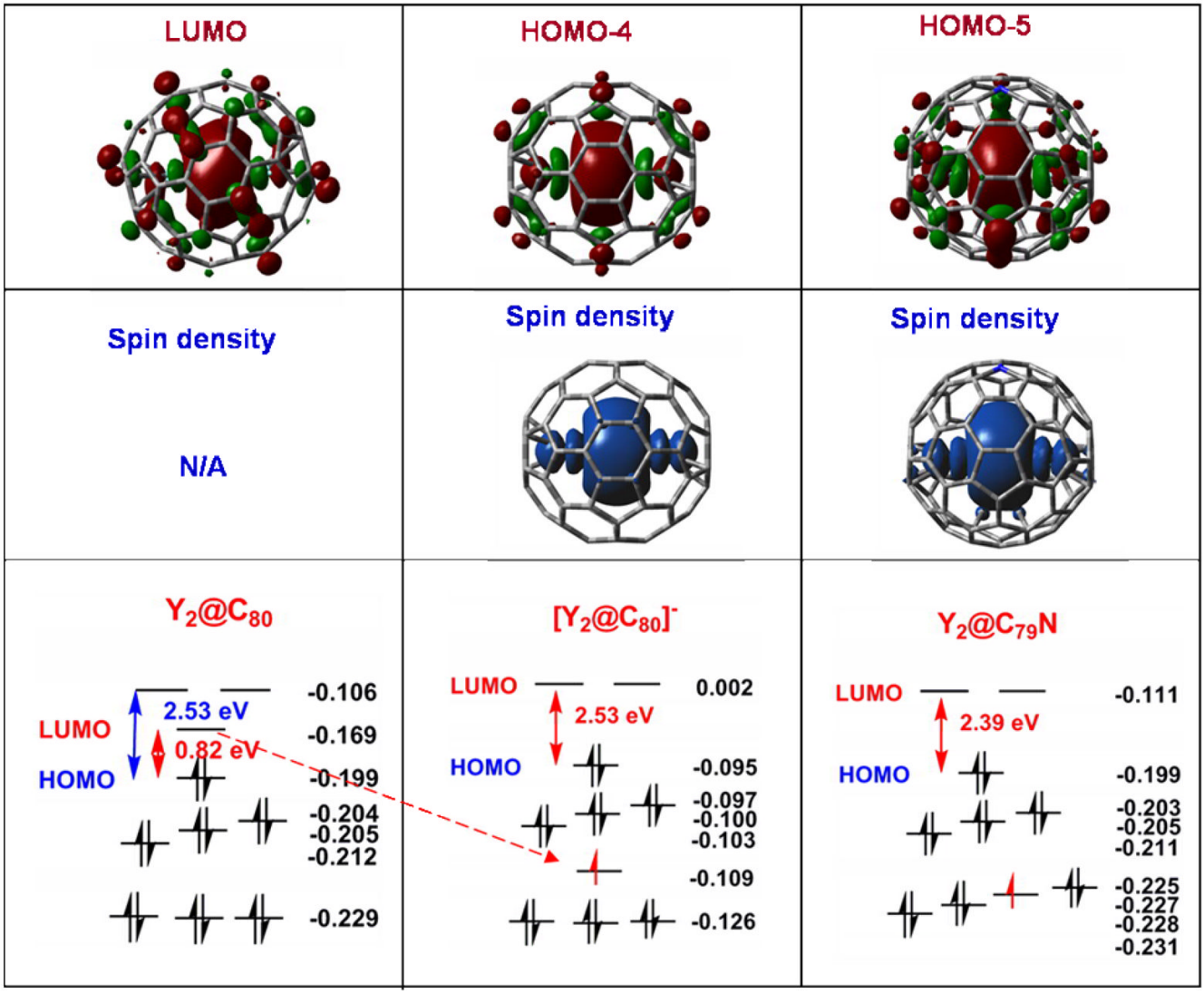

Figure 5.

Kohn-Sham UB3LYP/DZVP(Y)+6-31G*(C,N) molecular orbitals for the optimized structures of $Y_2@I_h$-C_{80}, $[Y_2@I_h\text{-}C_{80}]^-$, and $Y_2@C_{79}N$ molecules. Orbital energies are shown at the bottom (energies of beta LUMO of $[Y_2@I_h\text{-}C_{80}]^-$ and $Y_2@C_{79}N$ molecules are omitted), while drawings of the critical yttrium based orbitals that contains the free spin in the paramagnetic molecules are shown at the top along with drawings of the distribution of the spin density in $[Y_2@I_h\text{-}C_{80}]^-$ and $Y_2@C_{79}N$.

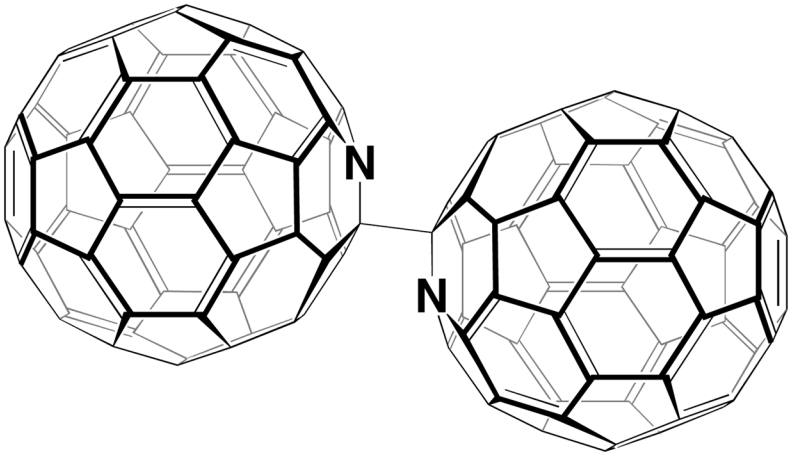

$\{C_{59}N\}_2$

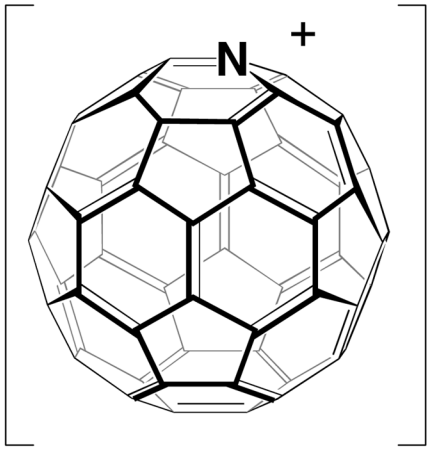

$[C_{59}N]^+$

Scheme 1.
Azafullerenes